

Two distinct metacommunities characterize the gut microbiota in Crohn's disease patients

Qing He^{1,2,3†}, Yuan Gao^{4,5†}, Zhuye Jie^{4,5}, Xinlei Yu^{4,5}, Janne Marie Laursen⁶, Liang Xiao^{4,5}, Ying Li¹, Lingling Li², Faming Zhang⁷, Qiang Feng^{4,8}, Xiaoping Li^{4,5}, Jinghong Yu^{4,5}, Chuan Liu^{4,5}, Ping Lan^{1,3}, Ting Yan², Xin Liu^{4,5}, Xun Xu^{4,5}, Huanming Yang^{4,9}, Jian Wang^{4,9}, Lise Madsen^{4,10,11}, Susanne Brix⁶, Jianping Wang^{1,3}, Karsten Kristiansen^{4,10*}, Huijue Jia^{4,5,12*}

* To whom correspondence should be addressed: K.K. (kk@bio.ku.dk) or H.J. (jiahuijue@genomics.cn)

† Contributed equally

¹Department of Gastroenterology, The Sixth Affiliated Hospital of The Sun Yat-sen University, Guangzhou 510610, China

²Department of nutrition, The Sixth Affiliated Hospital of Sun Yat-sen University, Guangzhou 510610, China

³Guangdong Provincial Key Laboratory of Colorectal and Pelvic Floor Diseases, the Sixth Affiliated Hospital, Sun Yat-sen University, Guangzhou 510610, China

⁴BGI-Shenzhen, Shenzhen 518083, China

⁵China National Genebank-Shenzhen, BGI-Shenzhen, Shenzhen 518083, China

⁶Department of Biotechnology and Biomedicine, Technical University of Denmark (DTU),

- 1 19 Kongens Lyngby, Denmark.
2
3
4 20 ⁷Digestive Endoscopy and Medical Center for Digestive Diseases, the Second Affiliated Hospital
5
6
7 21 of Nanjing Medical University, Nanjing 210011, Jiangsu Province, China
8
9
10
11 22 ⁸Shenzhen Engineering Laboratory of Detection and Intervention of Human Intestinal Microbiome,
12
13
14 23 BGI-Shenzhen, Shenzhen 518083, China
15
16
17 24 ⁹James D. Watson Institute of Genome Sciences, Hangzhou 310058, China
18
19
20
21 25 ¹⁰Laboratory of Genomics and Molecular Biomedicine, Department of Biology, University of
22
23
24 26 Copenhagen, Universitetsparken 13, 2100 Copenhagen, Denmark.
25
26
27
28 27 ¹¹National Institute of Nutrition and Seafood Research, Bergen, Norway.
29
30
31
32 28 ¹²Shenzhen Key Laboratory of Human Commensal Microorganisms and Health Research,
33
34
35 29 BGI-Shenzhen, Shenzhen 518083, China
36
37
38 30
39
40
41
42
43
44
45
46
47
48
49
50
51
52
53
54
55
56
57
58
59
60
61
62
63
64
65

1
2
3
4
5
6
7
8
9
10
11
12
13
14
15
16
17
18
19
20
21
22
23
24
25
26
27
28
29
30
31
32
33
34
35
36
37
38
39
40
41
42
43
44
45
46
47
48
49
50
51
52
53
54
55
56
57
58
59
60
61
62
63
64
65

51 **Keywords:** Crohn's disease, Gut microbe, Metagenomics, Exclusive enteral nutrition

1 **52 Background**

2
3
4 53 Crohn’s disease (CD) is an inflammatory bowel disease (IBD) that may affect any part of the
5
6
7 54 gastrointestinal (GI) tract. Gut microbes have recently gained much attention as plausible
8
9
10 55 drivers of CD. This notion is supported by the fact that the intimate interaction between the
11
12
13 56 gut microbiota and the intestinal mucosa constantly modulates and shapes the gut immune
14
15
16 57 system[1], and departure from the normal homeostatic microbiome state likely triggers
17
18
19 58 immune dysregulation via pro-inflammatory cues. Specific pathogens that possibly cause CD
20
21
22 59 have been identified, such as adherent-invasive *Escherichia coli* (AIEC) [2] and
23
24
25 60 *Mycobacterium avium paratuberculosis* (MAP) [3]. However, these bacteria were detected
26
27
28 61 only in a fraction of patients [2, 3]. It is therefore assumed that the overall composition of the
29
30
31 62 gut microbiota rather than specific microorganisms accounts for the inflammatory state in CD.
32
33
34 63 Studies using 16S rRNA gene amplicon sequencing to characterize CD-associated microbiota
35
36
37 64 abnormalities revealed an overall reduced microbial diversity in CD [1, 4, 5]. Moreover, a
38
39
40 65 reduction in the relative abundance of *Roseburia* [6], *Faecalibacterium* [1, 5-7],
41
42
43 66 *Bifidobacteriaceae* [1], and *Clostridiales* [5], and an increase in the relative abundance of the
44
45
46 67 *Enterobacteriaceae* family members [1, 4-7] were reported in patients with CD. However,
47
48
49 68 studies using 16S rRNA gene amplicon sequencing have limitations in taxonomic resolution
50
51
52 69 and functional inference. Metagenomic shotgun sequencing can overcome these limitations,
53
54
55 70 but only a few studies have applied metagenomic shotgun sequencing on CD microbiota,
56
57
58 71 including the initial report on 4 CD cases (along with 21 ulcerative colitis cases) to illustrate
59
60
61 72 the utility of the first gut microbial reference gene catalog[8], and a subsequent study on 23

1 73 pediatric CD patients[9]. The current incomplete understanding of the functional roles played
2
3 74 by the gut microbiota has limited the efforts to devise more targeted treatments.
4
5

6
7 75 Conventionally, CD is treated with anti-inflammatory or immunosuppressive medications, or
8
9 76 by surgery if symptoms cannot be improved pharmaceutically [10]. However, side effects and
10
11 77 complications such as infection and malnutrition accompany these treatments [11], which
12
13 78 imperil the patient's life. Although not widely used, exclusive enteral nutrition (EEN) is a
14
15 79 low-risk, non-invasive therapy for CD that involves exclusive ingestion of 100% liquid
16
17 80 formula made up of either elemental or polymeric nutrients [12]. In pediatric CD up to 85%
18
19 81 remission has been achieved by EEN [12]. Nevertheless, in adult CD, EEN has not delivered
20
21 82 desirable effectiveness, which to some extent may be attributed to non-adherence and
22
23 83 interpersonal variations in clinical conditions [12]. The mechanism underlying the alleviation
24
25 84 of CD by EEN also remains unclear, though nutritional improvement and microbial
26
27 85 involvement possibly play a role [13]. Although previous studies have described the effects of
28
29 86 EEN on the microbiota of pediatric CD[9, 14], it is unclear how EEN modulates their adult
30
31 87 counterpart.
32
33
34
35
36
37
38
39
40
41
42
43

44 88 Through metagenomic sequencing and data analysis, we herein provide novel insights into the
45
46 89 CD microbiota at both compositional and inferred functional levels. We identified two
47
48 90 metacommunity stages within CD patients that differed by abundance of gram-negative
49
50 91 pro-inflammatory bacteria and presence of genes involved in production of anti-inflammatory
51
52 92 short-chain fatty acids. In addition, we investigated the effect of short-term EEN on the CD
53
54 93 microbiota. Our study highlights the presence of two microbiota severity-states related to gut
55
56
57
58
59
60
61
62
63
64
65

1
2
3
4
5
6
7
8
9
10
11
12
13
14
15
16
17
18
19
20
21
22
23
24
25
26
27
28
29
30
31
32
33
34
35
36
37
38
39
40
41
42
43
44
45
46
47
48
49
50
51
52
53
54
55
56
57
58
59
60
61
62
63
64
65

94 microbiota dysbiosis in CD and indicates possible functional links between the microbiota
95 and the underlying immunological dysbalance in CD.

1 96 **Data Description**

2
3
4 97 49 CD patients and 54 healthy controls (CTs) were enrolled in this study. 14 CD patients
5
6
7 98 underwent EEN treatment (for the clinical profiles of CD patients, see Supplementary Table
8
9
10 99 1). Fecal samples were collected from all participants at baseline and from the EEN-treated
11
12
13 100 patients after two-week EEN treatment, totaling 117 fecal samples. After DNA extraction,
14
15 101 DNA library of an insert size of 350bp was constructed and then sequenced on an Illumina
16
17 102 HiSeq 2000 analyzer at BGI (Shenzhen, China) using 100bp paired-end (PE) sequencing. In
18
19
20
21 103 total, we generated ~700Gb raw data, and 672Gb of them remained after filtering out
22
23
24 104 low-quality or host reads. The dataset is available from the EBI Database (Accession No.
25
26 105 PRJEB15371)[15]. On average ~55.65 million high-quality reads per sample were generated
27
28
29 106 for further analyses. The proportion of high-quality reads among all raw reads from each
30
31
32 107 sample was 95.98% on average. Using both de novo assembly and alignment against the
33
34
35 108 integrated gene catalog (IGC) geneset, 2036584 genes with occurrence rate over 5% were
36
37
38 109 obtained.

39
40
41 110 **Analyses**

42
43
44
45 111 **Clustering of CD microbiota into distinct metacommunities**

46
47
48
49 112 When the gut microbiotas of CD patients were compared to their non-CD counterparts, both
50
51
52 113 microbial gene counts (**Supplementary Fig. 1a**) and diversity (**Supplementary Fig. 1b**) were
53
54
55 114 considerably lower in CD patients than in CTs. For high-confidence taxonomic identification,
56
57
58 115 co-abundant genes were binned into metagenomics species (MGS) [16] (harboring more than
59
60
61
62
63
64
65

1 116 700 genes) which were thereafter used for taxonomic annotation. A total of 452 MGS were
2
3 117 identified, with 151 of them being assigned to existing taxonomic entities (**Supplementary**
4
5
6 118 **Table 2**).

7
8
9
10 119 To capture the principal differences between non-CD and CD microbiome structures, we
11
12 120 adopted a combinatory approach which started with sample clustering based on the dirichlet
13
14
15 121 multinomial mixtures (DMM) model [17], followed by the identification of discriminative
16
17 122 microbes using an adapted version of the linear discriminant analysis (LDA) effect size
18
19 123 (LEfSe) method [18]. Based on Laplace approximation [17], we identified 3 clusters to exhibit
20
21 124 minimal negative log posterior (**Supplementary Fig. 1c**). Based on this we clustered the
22
23 125 microbiome samples of CD and CTs into 3 metacommunities (A, B and C), which displayed
24
25 126 intra-community homogeneity and inter-community dissimilarity (**Fig. 1a**). The membership
26
27 127 of a metacommunity was associated with disease status (Fisher's exact test with BH
28
29 128 adjustment, $q < 0.01$, **Supplementary Table 3**). Metacommunity A was dominated by CT
30
31 129 samples and metacommunity C exclusively by CD samples, whereas metacommunity B
32
33 130 contained both CT and CD samples (**Fig. 1a**). Based on a less stringent LEfSe method, 85
34
35 131 MGS were identified as discriminative microbes for the metacommunities or sub-groups (CT
36
37 132 and CD groups within metacommunity B) (**Fig. 1a** and **Supplementary Table 4**). The
38
39 133 majority of metacommunity A-enriched MGS were reduced in metacommunity B and further
40
41 134 depleted in C, including short-chain fatty acid (SCFA)-producing bacteria such as
42
43 135 *Bifidobacterium* species, *Faecalibacterium prausnitzii*, *Alistipes shahii* and *Roseburia* species
44
45
46
47
48
49 136 (**Fig. 1a** and **Supplementary Table 4**). Among others, SCFA-producing bacteria *Bacteroides*
50
51
52
53
54
55
56
57
58
59
60
61
62
63
64
65

1 137 *cellulosilyticus*, *Bacteroides xylanisolvens*, and *Clostridium nexile*, a member of the
2
3
4 138 immunomodulatory Clostridium cluster XIVa [19], were enriched in metacommunity B (**Fig.**
5
6 139 **1a** and **Supplementary Table 4**). Another Clostridium cluster XIVa clade member,
7
8
9 140 *Clostridium symbiosum*, and a number of opportunistic pathogens such as *E. coli*, *Klebsiella*
10
11 141 *pneumoniae*, *Streptococcus salivarius*, and *Clostridium bolteae* were overrepresented in
12
13
14 142 metacommunity C (**Fig. 1a** and **Supplementary Table 4**), suggesting that subjects in this
15
16
17 143 group had impaired ability to suppress colonization by pathogenic species in their gut. We
18
19
20 144 also evaluated whether metacommunities differed in the degree of dysbiosis associated with
21
22
23 145 CD through computing the Microbial Dysbiosis index (MD-index) [5]. CD microbiotas from
24
25
26 146 metacommunity C had significantly higher values of the MD-index than those from
27
28
29 147 metacommunity B ($p = 7.63e-05$, **Fig. 1a** and **Supplementary Table 1**), suggesting a more
30
31
32 148 severe degree of dysbiosis in this CD subgroup. Combined, these compositionally distinct
33
34
35 149 metacommunities recapitulate disparate configurations of the microbiota under normal and
36
37 150 CD conditions.

38
39
40 151 The separation of microbiomes into metacommunities was confirmed by principal coordinate
41
42
43 152 analysis (PCoA), which clustered samples by both metacommunity identity and disease status
44
45
46 153 (**Fig. 1b**). We determined whether the variations in microbiome composition were
47
48
49 154 accompanied with clinical phenotypes. In CD patients, 23 clinical variables together with age
50
51
52 155 correlated with microbiome variation, with uric acid (UA) and blood leukocyte numbers
53
54
55 156 being the top two covariates (effect size > 0.2) (**Supplementary Fig. 2b**). When categorized
56
57 157 into groups, various plasma biomarkers, including inflammatory markers were the strongest
58
59
60
61
62
63
64
65

1 158 classes of covariates (effect size > 0.2) (**Supplementary Fig. 2c**). However, despite the
2
3 159 existence of microbiome variations and their correlation with clinical states, no significant
4
5
6 160 differences were detected for these clinical variables between metacommunity B and C CD
7
8
9 161 patients (**Supplementary Fig. 2d**).

10
11
12 162

13 14 15 16 163 **CD- and metacommunity-associated functional traits**

17
18
19
20 164 We next analyzed the functional changes associated with disease status and differences in
21
22
23 165 microbiome structure. We made pair-wise comparisons after performing functional annotation
24
25
26 166 using the Kyoto Encyclopedia of Genes and Genomes (KEGG) database (KEGG,
27
28
29 167 RRID:SCR_012773). A large number of CD- and metacommunity-related functional shifts
30
31
32 168 were identified at the level of pathways and modules (**Fig. 2a, Supplementary Table 5** and
33
34 169 **Supplementary Table 6**). We observed consistent changes in CD microbiotas in all within- or
35
36
37 170 between- metacommunity comparisons (in B-CD vs A-CT, C-CD vs A-CT, B-CD vs B-CT,
38
39
40 171 and C-CD vs B-CT) (**Fig. 2a**). The composition of the microbiota of CD patients indicated
41
42
43 172 consistent changes in the potential for carbohydrate utilization compared to the CT
44
45
46 173 counterparts with a decreased abundance of pathways involved in starch and sucrose
47
48
49 174 metabolism, and enrichment of pathways involved in simple carbon metabolism such as
50
51
52 175 fructose, mannose, and galactose in the microbiota of CD patients (**Fig. 2a**). In addition, we
53
54
55 176 observed an enrichment of genes in pathways involved in glyoxylate, dicarboxylate,
56
57
58 177 propanoate and butanoate metabolism as well as in pathways involved in transport of simple
59
60
61 178 sugars (phosphotransferase system) (**Fig. 2a**). Interestingly, the reporter scores of numerous

1 179 amino acid metabolic pathways exhibited marked decreases or increases in CD patients
2
3 180 compared to CTs, suggesting possible significant changes in the amino acid metabolic profiles
4
5
6 181 (**Fig. 2a**). Of note, the potential for methane metabolism was also diminished in CD patients
7
8
9 182 (**Fig. 2a**). By contrast, microbes in CD patients exhibited enhanced potential for xenobiotic
10
11
12 183 degradation (e.g. of toluene, fluorobenzoate, styrene, benzoate, dioxin, and xylene) and
13
14
15 184 antioxidant defense (e.g. ascorbate, aldarate and glutathione metabolism) (**Fig. 2a**). In parallel,
16
17
18 185 a number of pathways associated with pathogenesis and virulence, including ABC
19
20
21 186 transporters, bacterial secretion system, and general LPS biosynthesis exhibited an
22
23
24 187 incremental enrichment from metacommunity A to C (**Fig. 2a**).
25
26
27 188 LPS, an inherent component of Gram-negative bacteria, is an endotoxin that can have
28
29
30 189 opposing effects on the immune response [20]. Since pathway and module analyses showed
31
32
33 190 an enrichment of general LPS biosynthesis in the CD microbiome (**Fig. 2a**), we took a novel
34
35
36 191 approach and investigated the capacity amongst all Gram-negative bacteria to produce the
37
38
39 192 pro-inflammatory hexa-acylated LPS as compared to the antagonizing silencing
40
41
42 193 penta-acylated LPS variant [21, 22]. We listed bacteria with a potential for synthesizing each
43
44
45 194 LPS variant (**Supplementary Table 7**) and compared the abundances of these bacteria
46
47
48 195 (**Supplementary Table 8**). The hexa-acylated LPS producing bacteria, *E. coli* and
49
50
51 196 *Morganella morganii* exhibited higher abundance in CD patients from metacommunity C
52
53
54 197 compared to non-CD individuals from metacommunity A (**Supplementary Table 7**).
55
56
57 198 Consistently, compared to metacommunity A (CT), microbes in metacommunity C (CD)
58
59
60 199 tended to produce LPS in a higher hexa- to penta-ratio, suggested by the increase in
61
62
63 200 abundance of bacteria with the hexa- over the penta-acetylated LPS variant (**Fig. 2b**), which

1 201 in part may account for an increased inflammatory stimulation of the CD gut.
2
3
4 202 The abundances of Gram-positive bacteria were reduced in metacommunity C, and in
5
6
7 203 metacommunity B as compared to CTs (**Fig. 2b**). These bacteria make up the largest reservoir
8
9
10 204 for production of SCFAs. SCFAs are not only colonotrophic nutrients but also
11
12
13 205 immunoregulatory molecules [23] that may reduce pro-inflammatory cues within the gut
14
15
16 206 environment. We estimated the abilities of the metacommunities to produce the SCFAs acetic
17
18
19 207 acid, propionic acid and butyric acid. This was done based on the presence of the genes
20
21
22 208 encoding the last enzyme within the respective biosynthetic pathway, thereby providing an
23
24
25 209 alternative method for predicting the capacity for biosynthesis of the bioactive end products
26
27
28 210 than that used in **Fig. 2a**, which was based on presence of genes involved in overall metabolic
29
30
31 211 pathways. Bacteria with a potential to produce SCFAs are listed in **Supplementary Table 7**.
32
33
34 212 Evidently, CD microbiotas, particularly those in metacommunity C, showed a decreased
35
36
37 213 abundance of key genes for SCFA production, including acetic acid, propionic acid and
38
39
40 214 butyric acid, when compared to the CT microbiota in metacommunity A (**Fig. 2c**).
41
42
43 215 Concordantly, the abundance of many SCFA-producing bacteria differed between CT and CD
44
45
46 216 samples (**Supplementary Table 8**). Thus, the gut microbiota in CD patients likely produces a
47
48
49 217 suboptimal amount of SCFAs compared to the healthy state.

50 218

51 52 53 219 **Disruption of normal gut microbial ecosystem and bacterial growth rate in CD**

54
55
56
57 220 The structure of a microbiota is the result of dynamic interactions between community
58
59
60

1 221 members. We generated correlation-based microbial interaction networks using the SparCC
2
3 222 algorithm (**Fig. 3, Supplementary Fig. 3**). Since metacommunity A and C were
4
5
6 223 representative of the typical CT and CD states, respectively, we first compared the
7
8
9 224 microbiome networks of these two groups (**Fig. 3a and 3b**). The control microbiota in
10
11
12 225 metacommunity A was characterized by a complex network of interactions between different
13
14 226 taxa, especially within or between the dominant phyla Bacteroidetes and Firmicutes (**Fig. 3a**).
15
16
17 227 However, the vast majority of these relationships was no longer significant in the CD patients
18
19
20 228 harboring metacommunity C (**Fig. 3b**). Among the strong interactions lost in the gut
21
22
23 229 microbiota of the C-CD group were positive correlations ($r>0.5$) of *Bacteroides*
24
25 230 *cellulosilyticus* with *Bacteroides thetaiotaomicron* and *Bacteroides* sp., and of *Ruminococcus*
26
27
28 231 *bromii* with *Eubacterium ventriosum* (**Fig. 3**). Only one new strong correlation was formed
29
30
31 232 between two unidentified taxa in the C-CD group (**Fig. 3**). Thus, the CD microbiota of
32
33
34 233 metacommunity C showed not only alterations in composition, but also reduced
35
36 234 interrelationships. In comparison, CT and CD microbiotas from metacommunity B did not
37
38
39 235 differ significantly in terms of network complexity, although numerous inter-taxon
40
41
42 236 relationships were altered (**Supplementary Fig. 3**).

43
44
45 237 Changes in bacterial growth rate may contribute to alterations in community structures. We
46
47
48 238 calculated the growth rate from the number of sequencing reads covering the replication
49
50
51 239 origin relative to reads covering the replication termination site [24]. Compared to CTs in
52
53
54 240 metacommunity A, the growth rate of many beneficial taxa decreased in metacommunity C,
55
56
57 241 including the SCFA-producing bacteria *Alistipes finegoldii*, *Alistipes shahii*, *Eubacterium*

1 242 *rectale*, *Roseburia intestinalis*, and several *Faecalibacterium prausnitzii* strains (**Fig. 3** and
2
3 243 **Supplementary Table 9**). Interestingly, certain pathogenic or opportunistic pathogenic
4
5
6 244 bacteria exhibiting an increased abundance in the C-CD group showed high growth rates (*E.*
7
8
9 245 *coli*, *Klebsiella pneumoniae*, *Bacteroides fragilis*, and *Streptococcus salivarius*) (**Fig. 3** and
10
11 246 **Supplementary Fig. 4** and **Supplementary Table 9**). Thus, differences in growth rate likely
12
13
14 247 contribute to the alterations in the relative abundance of bacteria in CTs and CD patients,
15
16
17 248 since the observed increase or decrease in growth rates largely concurred with their changes
18
19
20 249 in relative abundance in CD samples (**Supplementary Fig. 4**). The reduction of growth rates
21
22
23 250 for most bacteria in the C-CD group may also be an indicator that this metacommunity
24
25
26 251 structure is unlikely to shift towards increased diversity over time without specific
27
28
29 252 intervention.

30 31 32 253 **Limited remodeling of CD microbiota composition by short-term EEN**

33
34
35
36 254 Fourteen patients in our cohort underwent EEN treatment after baseline sampling and
37
38
39 255 provided fecal samples after two weeks of treatment. We assessed whether short-term EEN
40
41
42 256 was sufficient to alter the microbiome structure in CD patients. For all patients but one
43
44 257 (GZCD029, marked by * in **Fig. 4b**), such short time intervention proved insufficient to
45
46
47 258 change their metacommunity identities (**Fig. 4a**), in accord with no significant change in
48
49
50 259 MD-indices ($p = 0.20$, **Fig. 4a** and **Supplementary Table 1**). However, moderate changes
51
52
53 260 occurred as illustrated by the shift in the relative position of microbiomes along the two
54
55
56 261 principal coordinates within pre-identified clusters (**Fig. 4b**).

57
58
59 262 Despite the limited remodeling of the overall microbiota composition, two-weeks EEN did

1 263 induce a variety of functional alterations (**Fig. 4c**, and **Supplementary Table 12** and
2
3 **Supplementary Table 13**). In a reverse manner to CD-associated shifts, functions such as
4
5
6 265 LPS biosynthesis and bacterial secretion system became less enriched, while starch and
7
8
9 266 sucrose metabolism and flagellar assembly were enhanced after EEN (**Fig. 4c**), suggesting a
10
11
12 267 partial functional recovery. However, certain CD-driven changes, such as functions associated
13
14
15 268 with ribosomes, one carbon folate pool, PTS, and ABC transporters, were exacerbated after
16
17
18 269 two-weeks EEN (**Fig. 4c**), indicating either side effects or temporal disease progression.
19
20
21 270 Nevertheless, short-term EEN did not affect the abundances of LPS- or SCFA-producing
22
23
24 271 bacteria (**Fig 4d, e, Supplementary Table 10**) nor their growth rates (**Supplementary Table**
25
26
27 272 **11**). However, network re-wiring occurred (**Supplementary Fig. 5**). Rather than interacting
28
29
30 273 with Firmicutes, bacteria from Bacteroidetes tended to interact with each other after EEN
31
32
33 274 treatment (**Supplementary Fig. 5**). By contrast, a majority of Firmicutes in patients after
34
35
36 275 EEN treatment presented more inter-dependences with Proteobacteria and unclassified
37
38
39 276 species compared to those before treatment (**Supplementary Fig. 5**). Overall, the CD
40
41
42 277 microbiota appeared relatively stable and refractory to two-week EEN intervention. Future
43
44
45 278 studies will need to determine if a longer intervention period with EEN will result in
46
47
48 279 restoration of normal functional microbiota in CD patients.
49
50
51
52
53
54
55
56
57
58
59
60
61
62
63
64
65

1 **281 Discussion**

2
3
4 282 Comparative metagenomic analysis of fecal samples from CD and healthy controls revealed
5
6
7 283 pronounced global alterations in the fecal microbiota of CD patients, characterized by two
8
9
10 284 distinct CD metacommunities comprising gradually limited bacterial diversity, by functional
11
12
13 285 aberrations towards a pronounced pro-inflammatory phenotype, and by structural
14
15
16 286 derangements of ecosystem networks.

17
18
19 287 Metacommunities constitute a robust means to distinguish microbiotas with different traits
20
21
22 288 and of distinct natures. Suggested by their signature microbes (the leverage between
23
24
25 289 beneficial bacteria or opportunistic pathogens) and supported by the MD-index,
26
27
28 290 metacommunity A might be representative of the healthy gut, while metacommunity B and C
29
30
31 291 likely represented a moderately imbalanced and a more pro-inflammatory state associated
32
33
34 292 with CD, respectively. Since the commensal microbiota is closely linked to the health of the
35
36
37 293 host, the classification of metacommunities is a novel promising tool to stratify patients based
38
39
40 294 on their microbiome configuration.

41 295 Our study identified systematic functional alterations of CD microbiome that reflected the
42
43
44 296 stressful microenvironment of the CD gut and its predisposition to inflammation. In this
45
46
47 297 respect, the decline in the potential for the biosynthesis of all SCFAs, which may modulate
48
49
50 298 the activation of the immune system and temper inflammation [25, 26], and the appearance of
51
52
53 299 microbes producing the pro-inflammatory hexa-acetylated LPS [20] are salient manifestations
54
55
56 300 of the inflammation-prone nature of the CD microbiota. Although LPS has long been
57
58
59 301 established as a pathogen-associated molecular pattern (PAMP) that triggers immune cascades

1 302 [20], it was more recently established that only the hexa-acylated LPS variant is able to
2
3 303 activate pro-inflammatory cues via TLR4 in humans [22], while the penta-acylated LPS
4
5
6 304 variant acts as an antagonist [21]. Our finding that the CD microbiota of metacommunity C
7
8
9 305 was enriched in microbes producing hexa-acylated LPS is consistent with previous
10
11
12 306 observations of the increased abundance of the *Enterobacteriaceae* family members in CD [1,
13
14
15 307 4-7], which are known to stimulate inflammation [27]. Together, these changes may severely
16
17
18 308 affect the host immune system, leading to an unchecked inflammatory state in CD. The
19
20
21 309 reduction in the network complexity of the CD microbiota of metacommunity C reinforced
22
23
24 310 the view that a globally disturbed microbial ecosystem may contribute to this disease. The
25
26
27 311 loss of reciprocal and cross-inhibitory relationships may impair the survival of beneficial
28
29
30 312 microbes and create favorable conditions for the blooming of pathogens. Likewise, it appears
31
32
33 313 to limit the growth of many gut bacteria found in healthy individuals. In this regard,
34
35
36 314 reconstruction of the normal ecosystem and not only the mere introduction of a single or
37
38
39 315 several commensal microbes may be needed to curb CD. In the case of EEN, a longer term of
40
41
42 316 treatment may be needed to achieve this goal. Analysis of the fecal microbiota is widely used
43
44
45 317 as a proxy for studying the gut microbiota composition because of the easiness and
46
47
48 318 noninvasive nature of fecal sampling, and has through the years resulted in deepening the
49
50
51 319 understanding of the relationship between the gut microbiota and IBD [1, 28]. However, new
52
53
54 320 avenues of sampling procedures open up for more comprehensive insights into the role played
55
56
57 321 by the intestinal location of microbial species (luminal or mucosal layer attachment to the
58
59
60 322 small and the large intestine) that, in combination with metagenomic sequencing, would allow
61
62
63
64
65

1 323 for deeper insights into the inter-individual diversity in ecological dysbalance in CD patients
2
3 324 in future studies.

4
5
6 325 Taken together, our metagenome-scale characterization of the CD gut microbiome supports
7
8 326 the notion of a shift towards enhanced pro-inflammatory capacity, which is most pronounced
9
10 327 in individuals harboring the severe-state metacommunity C. The level of details in this
11
12 328 analysis, also encompassing yet unannotated bacteria, may pave the way for elucidating
13
14 329 microbial disturbances predictive for CD by enabling the discovery of composite microbial
15
16 330 CD biomarkers. In addition, it may allow for the identification of future therapeutic targets
17
18 331 based on microbiota signatures, thereby implementing personalized medicine to CD patients
19
20 332 based on the individual microbiome composition.
21
22
23
24
25
26

27
28 333

29 30 31 32 334 **Methods**

33 34 35 36 335 **Study cohort, EEN treatment and sample collection**

37
38
39 336 49 CD patients and 54 healthy controls were enrolled in this study at the Sixth Affiliated
40
41 337 Hospital of the Sun Yat-sen University, Guangdong, China. All patients met the diagnostic
42
43 338 criteria for CD, according to the Montreal classification system [29]. Patients diagnosed with
44
45 339 diabetes, tumor, cardiovascular, kidney, liver, and metabolic diseases were excluded from this
46
47
48 340 study.
49
50
51

52
53 341

54
55
56 342 Among these participants, 14 CD patients underwent EEN treatment. ENSURE® (Abbott
57
58 343 Laboratories, Abbott Park, USA), PEPTISON®, NUTRISON POWDER® (NUTRICIA,

1 344 Danone, Netherlands) and FRESUBIN® (Sino-Swed Pharmaceutical Corp. Ltd, China) were
2
3 345 used as the standard oral polymeric formulas, and their ingredients are detailed in
4
5
6 346 Supplementary Table 14. Patients chose from these formulas, with 8 patients selecting
7
8
9 347 ENSURE® and the others selecting a mixture of two or more formulas. Formulas were
10
11
12 348 consumed at 30 kcal/kg per day as the sole nutrient source. Patients who adhered to EEN
13
14 349 treatment had their lesion healed.

15
16
17 350

18
19
20 351 Fecal samples were collected from all participants at baseline (n=103), and from the
21
22 352 EEN-treated CD patients after 2 weeks of treatment (n=14), totaling 117 samples. The fecal
23
24
25 353 samples were immediately frozen and stored at -80°C until being processed. DNA extraction
26
27
28 354 was performed according to the protocols described previously [30].

29
30 355

31 32 33 34 35 356 **Metagenomic sequencing and assembly**

36
37
38 357 Paired-end metagenomic sequencing was conducted on the Illumina platform (insert size, 350
39
40
41 358 bp; read length, 100 bp). Quality control was performed and adaptor and host contamination
42
43
44 359 were filtered. Sequencing reads were de novo assembled into contigs with SOAPdenovo
45
46
47 360 v2.04 [31] (SOAPdenovo2, RRID:SCR_014986) as described previously [30].

48
49 361

50 51 52 53 362 **Co-abundance gene groups identification and functional annotation**

1 363 Applying the metagenomic species (MGS) clustering method[16], we clustered genes
2
3 364 according to their co-variations in abundance across samples. A group of co-abundant genes
4
5
6 365 was identified as a MGS if it contained 700 or more genes. These MGS were subjected to
7
8
9 366 subsequent analysis. Taxonomic assignment of the mapped genes was performed according to
10
11 367 the Integrated Microbial Genomes (IMG, v400) database using an in-house pipeline detailed
12
13 368 previously[30], with 70% overlap and 65% identity for assignment to phylum, 85% identity to
14
15 369 genus, and 95% identity to species. The relative abundance of a co-abundance gene group was
16
17 370 calculated from the relative abundance of its genes.
18
19
20
21

22 371 Differentially enriched KO pathways or modules were identified according to their reporter
23
24
25 372 scores[32], which were calculated from the Z-scores of individual KOs.
26
27

28 373 We assessed the production capacity for the two LPS forms based on the abundances of genes
29
30 374 of the entire lipid A biosynthesis pathway, and separated them into penta-acylated LPS
31
32 375 producers (harboring all lipid A pathway genes except for LpxM), and pro-inflammatory
33
34 376 hexa-acylated LPS producers (all lipid A pathway genes). MGS with no lipid A pathway
35
36 377 genes were assigned as Gram-positive bacteria.
37
38
39
40
41

42 378 Sequences of SCFA-producing enzymes were retrieved as previously described [33]. Genes in
43
44 379 the reference gut microbiome gene catalog[8] were identified as these enzymes (best match
45
46 380 according to BlastP (BLASTP, RRID:SCR_001010), identity > 35%, score > 60, E<1e-3), and
47
48 381 their relative abundances could then be determined accordingly.
49
50
51
52

53 382

54
55 383 **α -Diversity and gene count**
56
57
58
59
60
61
62
63
64
65

1 384 α -Diversity (within-sample diversity) was calculated on the basis of the gene profile of each
2
3 385 sample according to the Shannon index as described previously [30]. The total gene count in
4
5
6 386 each fecal sample was determined as in ref.[34]. Genes with at least one mapped read were
7
8
9 387 considered present.

10
11 388

12 13 14 15 389 **PERMANOVA of the influence of clinical and lifestyle factors**

16
17
18
19 390 Permutational multivariate analysis of variance (PERMANOVA) [30] was performed on the
20
21
22 391 gene-abundance profiles of the samples to assess the effect of each of the factors listed in
23
24
25 392 Table 1. We used Bray-Curtis distance and 9,999 permutations in R (3.10, vegan package, R
26
27 393 Project for Statistical Computing, RRID:SCR_001905) [35].

28
29
30 394

31 32 395 **Details of updated LefSe algorithm**

33
34
35
36
37 396 Differential abundance analyses were performed using a less stringent LefSe algorithm to
38
39
40 397 identify feature microbes whose abundances differed at least in one comparison[5].
41
42
43 398 Metacommunities and subgroups in metacommunity B were included for comparisons. The
44
45 399 biomarker relevance was ranked according to bootstrapped (n=30) logarithmic linear
46
47
48 400 discriminant analysis scores of at least 2. The open source R code is available at
49
50
51 401 <https://github.com/andriaYG/LDA-EffectSize>.

52
53 402

54 55 56 57 403 **Effect size analysis**

1 404 24 metadata covariates and their combined effect size when pooled into the broader
2
3 405 predefined categories (blood fat, coagulation, inflammation markers, and plasma biomarkers)
4
5
6 406 was estimated with the *bioenv* function in the vegan R package, which selects the
7
8
9 407 combination of covariates with strongest correlation to microbiota variation (Pearson
10
11
12 408 correlation between Gower distances of covariates and microbiome Bray-Curtis dissimilarity,
13
14 409 Supplementary Fig. 2A).
15

16
17 410

21 411 **Correlation network inferred by phylogenetic marker genes**

22
23 412 Eighty-five MGS, which were previously selected via the detection of microbial community
24
25
26 413 clusters through DMM modelling, were subjected to compositionality data analysis using the
27
28
29 414 SparCC algorithm[36]. Taxon–taxon correlation coefficients were estimated as the average of
30
31
32 415 20 inference iterations with the strength threshold of 0.25. Correlations with the
33
34
35 416 corresponding empirical P values less than 0.01 were retained, which was calculated via a
36
37
38 417 total of 10,000 simulated data sets. This set of iterative procedures was applied separately to
39
40
41 418 data from CTs and CD patients, and to patients’ data before and after EEN to infer the
42
43
44 419 correlation values. Correlation coefficients with magnitude of 0.3 or above were selected for
45
46 420 visualization in Cytoscape (version 3.3.0, Cytoscape, RRID:SCR_003032).
47

48
49 421

51 422 **Availability of supporting data**

1 423 The raw sequencing data can be found in the EBI database, under the BioProject number
2
3
4 424 PRJEB15371 [15]. The data sets supporting the results of this article are available in the
5
6 425 GigaDB repository [37].
7

8 9 426 **List of abbreviations**

10
11 427 CD, Crohn's disease; CT, controls; EEN, exclusive enteral nutrition; IBD, inflammatory
12
13 428 bowel disease; GI, gastrointestinal; AIEC, adherent-invasive *Escherichia coli*; MAP,
14
15 429 *Mycobacterium avium paratuberculosis*; MGS, metagenomics species; LDA, linear
16
17 430 discriminant analysis; LEfSe, linear discriminant analysis effect size; MD-index, microbial
18
19 431 dysbiosis index; PCoA, principal coordinate analysis; UA, uric acid; KEGG, Kyoto
20
21 432 Encyclopedia of Genes and Genomes; LPS, lipopolysaccharide; SCFA, short-chain fatty acid;
22
23 433 PAMP, pathogen-associated molecular pattern; IMG, Integrated Microbial Genomes.
24
25
26
27
28
29
30

31 434 **Consent for publication**

32
33
34 435 This study was approved by both the institutional review boards at Sixth Affiliated Hospital of
35
36 436 Sun Yat-sen University and the BGI ethics committee. All protocols were conducted in
37
38
39 437 compliance with the Declaration of Helsinki and explicit informed consent was obtained from
40
41
42 438 all participants.
43

44 439 **Competing interests**

45
46
47 440 The authors declare that they have no competing interests
48
49

50 441 **Funding**

51
52
53 442 This research was supported by the National Natural Science Foundation of China (grant No.
54
55 443 81470795 and 81670606), the Shenzhen Municipal Government of China (grant No.
56
57 444 JSGG20160229172752028 and JCYJ20160229172757249).
58
59
60

1 445

2
3 446 **Authors' contributions**

4
5
6 447 All authors read and approved the final manuscript. Q.H., Jian W., Huanming Y., X.X. and
7
8
9 448 X.L. conceived the study. Q.H. participated in the design of the study. L.X., Y.L., L.L, Faming
10
11
12 449 Z., Q.F., Xiaoping L., J.Y., C.L., J.C., and T.Y. carried out the sample collection and
13
14
15 450 preparation. Y.G. and Z.J. participated in sequence assembly, gene mapping and MGS
16
17
18 451 identification. J.M.L. and S.B. performed the analysis of LPS variants. Z.J. generated the
19
20
21 452 SCFA abundance profile. Y.G. carried out the bioinformatics analysis of metacommunities,
22
23
24 453 functions and networks. Y.G., X.Y., L.M, S.B., K.K. and H.J. wrote the manuscript. K.K., S.B.
25
26 454 and H.J. supervised project.

27
28 455 **Acknowledgements**

29
30
31 456 We gratefully acknowledge colleagues at BGI-Shenzhen for DNA extraction, library
32
33
34 457 construction, sequencing, and discussions.

35
36
37 458
38
39 459 **References**

- 40
41
42
43 460 1. Imhann F, Vich Vila A, Bonder MJ, Fu J, Gevers D, Visschedijk MC, Spekhorst LM,
44
45 461 Alberts R, Franke L, van Dullemen HM *et al.* **Interplay of host genetics and gut**
46
47 462 **microbiota underlying the onset and clinical presentation of inflammatory bowel**
48
49 463 **disease.** *Gut* 2016.
50
51
52
53
54 464 2. Barnich N, Darfeuille-Michaud A: **Adherent-invasive Escherichia coli and Crohn's**
55
56 465 **disease.** *Curr Opin Gastroenterol* 2007, **23**:16-20.
57
58
59
60
61
62
63
64
65

1 466 3. Hermon-Taylor J, Bull TJ, Sheridan JM, Cheng J, Stellakis ML, Sumar N: **Causation of**
2
3 467 **Crohn's disease by Mycobacterium avium subspecies paratuberculosis.** *Can J*
4
5
6 468 *Gastroenterol* 2000, **14**:521-539.
7
8
9 469 4. Ricanek P, Lothe SM, Frye SA, Rydning A, Vatn MH, Tonjum T: **Gut bacterial profile in**
10
11 470 **patients newly diagnosed with treatment-naive Crohn's disease.** *Clin Exp*
12
13 471 *Gastroenterol* 2012, **5**:173-186.
14
15
16
17 472 5. Gevers D, Kugathasan S, Denson LA, Vazquez-Baeza Y, Van Treuren W, Ren B,
18
19 473 Schwager E, Knights D, Song SJ, Yassour M *et al.* **The treatment-naive microbiome in**
20
21 474 **new-onset Crohn's disease.** *Cell Host Microbe* 2014, **15**:382-392.
22
23
24
25 475 6. Morgan XC, Tickle TL, Sokol H, Gevers D, Devaney KL, Ward DV, Reyes JA, Shah
26
27 476 SA, LeLeiko N, Snapper SB *et al.* **Dysfunction of the intestinal microbiome in**
28
29 477 **inflammatory bowel disease and treatment.** *Genome Biol* 2012, **13**:R79.
30
31
32
33 478 7. Thorkildsen LT, Nwosu FC, Avershina E, Ricanek P, Perminow G, Brackmann S, Vatn
34
35 479 MH, Rudi K: **Dominant fecal microbiota in newly diagnosed untreated inflammatory**
36
37 480 **bowel disease patients.** *Gastroenterol Res Pract* 2013, **2013**:636785.
38
39
40
41 481 8. Li J, Jia H, Cai X, Zhong H, Feng Q, Sunagawa S, Arumugam M, Kultima JR, Prifti E,
42
43 482 Nielsen T: **An integrated catalog of reference genes in the human gut microbiome.**
44
45 483 *Nature biotechnology* 2014, **32**:834-841.
46
47
48
49 484 9. Quince C, Ijaz UZ, Loman N, Eren AM, Saulnier D, Russell J, Haig SJ, Calus ST,
50
51 485 Quick J, Barclay A: **Extensive modulation of the fecal metagenome in children with**
52
53 486 **Crohn's disease during exclusive enteral nutrition.** *The American journal of*
54
55 487 *gastroenterology* 2015, **110**:1718-1729.
56
57
58
59
60
61
62
63
64
65

1 488 10. Torres J, Mehandru S, Colombel JF, Peyrin-Biroulet L: **Crohn's disease**. *Lancet* 2016.

2

3 489 11. Buchman AL: **Side effects of corticosteroid therapy**. *J Clin Gastroenterol* 2001,

4

5

6 490 **33:289-294**.

7

8

9 491 12. Wall CL, Day AS, Geary RB: **Use of exclusive enteral nutrition in adults with Crohn's**

10

11 492 **disease: a review**. *World J Gastroenterol* 2013, **19:7652-7660**.

12

13

14 493 13. Day AS, Lopez RN: **Exclusive enteral nutrition in children with Crohn's disease**. *World*

15

16 494 *J Gastroenterol* 2015, **21:6809-6816**.

17

18

19

20 495 14. Kaakoush NO, Day AS, Leach ST, Lemberg DA, Nielsen S, Mitchell HM: **Effect of**

21

22 496 **exclusive enteral nutrition on the microbiota of children with newly diagnosed Crohn's**

23

24 497 **disease**. *Clinical and translational gastroenterology* 2015, **6:e71**.

25

26

27

28 498 15. He Q GY, Jie Z, Yu X, Laursen JM, Xiao L, et al.: **The gut microbiome in Crohn's**

29

30 499 **disease and modulation by exclusive enteral nutrition**. In. EMBL-EBI; 2016.

31

32

33

34 500 16. Nielsen HB, Almeida M, Juncker AS, Rasmussen S, Li J, Sunagawa S, Plichta DR,

35

36 501 Gautier L, Pedersen AG, Le Chatelier E *et al*: **Identification and assembly of genomes**

37

38 502 **and genetic elements in complex metagenomic samples without using reference**

39

40 503 **genomes**. *Nat Biotechnol* 2014, **32:822-828**.

41

42

43

44 504 17. Holmes I, Harris K, Quince C: **Dirichlet multinomial mixtures: generative models for**

45

46 505 **microbial metagenomics**. *PLoS One* 2012, **7:e30126**.

47

48

49

50 506 18. Segata N, Izard J, Waldron L, Gevers D, Miropolsky L, Garrett WS, Huttenhower C:

51

52 507 **Metagenomic biomarker discovery and explanation**. *Genome Biol* 2011, **12:R60**.

53

54

55

56 508 19. Atarashi K, Tanoue T, Shima T, Imaoka A, Kuwahara T, Momose Y, Cheng G,

57

58 509 Yamasaki S, Saito T, Ohba Y *et al*: **Induction of colonic regulatory T cells by**

1 510 indigenou Clostridium species. *Science* 2011, **331**:337-341.

2

3 511 20. Raetz CR, Whitfield C: **Lipopolysaccharide endotoxins**. *Annu Rev Biochem* 2002,

4

5

6 512 **71**:635-700.

7

8

9 513 21. Park BS, Song DH, Kim HM, Choi B-S, Lee H, Lee J-O: **The structural basis of**

10

11 514 **lipopolysaccharide recognition by the TLR4-MD-2 complex**. *nature* 2009,

12

13

14 515 **458**:1191-1195.

15

16

17 516 22. Brix S, Eriksen C, Larsen JM, Bisgaard H: **Metagenomic heterogeneity explains dual**

18

19

20 517 **immune effects of endotoxins**. *Journal of Allergy and Clinical Immunology* 2015,

21

22 518 **135**:277.

23

24

25 519 23. Puertollano E, Kolida S, Yaqoob P: **Biological significance of short-chain fatty acid**

26

27

28 520 **metabolism by the intestinal microbiome**. *Current opinion in clinical nutrition and*

29

30 521 *metabolic care* 2014, **17**:139-144.

31

32

33

34 522 24. Korem T, Zeevi D, Suez J, Weinberger A, Avnit-Sagi T, Pompan-Lotan M, Matot E,

35

36 523 Jona G, Harmelin A, Cohen N *et al*: **Growth dynamics of gut microbiota in health and**

37

38

39 524 **disease inferred from single metagenomic samples**. *Science* 2015, **349**:1101-1106.

40

41

42 525 25. Furusawa Y, Obata Y, Fukuda S, Endo TA, Nakato G, Takahashi D, Nakanishi Y,

43

44 526 Uetake C, Kato K, Kato T *et al*: **Commensal microbe-derived butyrate induces the**

45

46

47 527 **differentiation of colonic regulatory T cells**. *Nature* 2013, **504**:446-450.

48

49

50 528 26. Singh N, Gurav A, Sivaprakasam S, Brady E, Padia R, Shi H, Thangaraju M, Prasad

51

52 529 PD, Manicassamy S, Munn DH *et al*: **Activation of Gpr109a, receptor for niacin and the**

53

54 530 **commensal metabolite butyrate, suppresses colonic inflammation and carcinogenesis**.

55

56

57

58 531 *Immunity* 2014, **40**:128-139.

59

60

61

62

63

64

65

- 1 532 27. Jensen SR, Mirsepasi-Lauridsen HC, Thyssen AH, Brynskov J, Krogfelt KA, Petersen
2
3 533 AM, Pedersen AE, Brix S: **Distinct inflammatory and cytopathic characteristics of**
4
5
6 534 **Escherichia coli isolates from inflammatory bowel disease patients.** *International*
7
8
9 535 *Journal of Medical Microbiology* 2015, **305**:925-936.
- 10
11 536 28. Round JL, Mazmanian SK: **The gut microbiota shapes intestinal immune responses**
12
13
14 537 **during health and disease.** *Nature Reviews Immunology* 2009, **9**:313-323.
- 15
16
17 538 29. Silverberg MS, Satsangi J, Ahmad T, Arnott IDR, Bernstein CN, Brant SR, Caprilli R,
18
19
20 539 Colombel J-F, Gasche C, Geboes K: **Toward an integrated clinical, molecular and**
21
22
23 540 **serological classification of inflammatory bowel disease: Report of a Working Party of**
24
25
26 541 **the 2005 Montreal World Congress of Gastroenterology.** *Canadian Journal of*
27
28
29 542 *Gastroenterology and Hepatology* 2005, **19**:5A-36A.
- 30
31 543 30. Qin J, Li Y, Cai Z, Li S, Zhu J, Zhang F, Liang S, Zhang W, Guan Y, Shen D: **A**
32
33
34 544 **metagenome-wide association study of gut microbiota in type 2 diabetes.** *Nature* 2012,
35
36
37 545 **490**:55-60.
- 38
39 546 31. Luo R, Liu B, Xie Y, Li Z, Huang W, Yuan J, He G, Chen Y, Pan Q, Liu Y:
40
41
42 547 **SOAPdenovo2: an empirically improved memory-efficient short-read de novo**
43
44
45 548 **assembler.** *GigaScience* 2012, **1**:1.
- 46
47
48 549 32. Patil KR, Nielsen J: **Uncovering transcriptional regulation of metabolism by using**
49
50
51 550 **metabolic network topology.** *Proceedings of the National Academy of Sciences of the*
52
53
54 551 *United States of America* 2005, **102**:2685-2689.
- 55
56 552 33. Claesson MJ, Jeffery IB, Conde S, Power SE, O'Connor EM, Cusack S, Harris HM,
57
58
59 553 Coakley M, Lakshminarayanan B, O'Sullivan O *et al.* **Gut microbiota composition**

1 554 **correlates with diet and health in the elderly. *Nature* 2012, **488**:178-184.**

2

3 555 34. Le Chatelier E, Nielsen T, Qin J, Prifti E, Hildebrand F, Falony G, Almeida M,

4

5

6 556 Arumugam M, Batto J-M, Kennedy S: **Richness of human gut microbiome correlates**

7

8

9 557 **with metabolic markers. *Nature* 2013, **500**:541-546.**

10

11 558 35. Zapala MA, Schork NJ: **Multivariate regression analysis of distance matrices for**

12

13

14 559 **testing associations between gene expression patterns and related variables.**

15

16

17 560 *Proceedings of the national academy of sciences* 2006, **103**:19430-19435.

18

19

20 561 36. Friedman J, Alm EJ: **Inferring correlation networks from genomic survey data.** *PLoS*

21

22 562 *Comput Biol* 2012, **8**:e1002687.

23

24

25 563 37. He Q GY, Jie Z, Yu X, Laursen JM, Xiao L, Li Y, Li L, Zhang F, Feng Q, Li X, Yu J, Liu

26

27

28 564 C, Lan P, Yan T, Liu X, Xu X, Yang H, Wang J, Madsen L, Brix S, Wang J, Kristiansen

29

30

31 565 K, Jia H. : **Supporting data for "Two distinct metacommunities characterize the gut**

32

33

34 566 **microbiota in Crohn's disease patients"** In. GigaScience Database. 2017.

35

36 567 <http://dx.doi.org/10.5524/100317>.

37

38

39 568

40

41

42

43

44

45

46

47

48

49

50

51

52

53

54

55

56

57

58

59

60

61

62

63

64

65

1 569 **Figure legends**

2
3
4 570 **Figure 1. Clustering of gut microbiota into metacommunities associated with CD. (a)**

5
6
7 571 Heatmap of signature microbes for three metacommunities determined by the DMM model.
8
9
10 572 Rows correspond to 85 discriminative MGS, with hierarchical clustering by their relative
11
12 573 abundances. Taxonomic annotations of these MGS are indicated at the right and colored by
13
14 574 phylum. Each column corresponds to one sample. The disease status (the first horizontal bar)
15
16 575 and metacommunity membership (the second horizontal bar) of samples are indicated by
17
18 576 color at the top, and MD index for each sample is represented by gray scale (the third
19
20
21
22 577 horizontal bar). **(b)** PCoA of the 85 MGS based on Jensen-Shannon distance (JSD). Colors
23
24 578 indicate metacommunity memberships, and shapes (triangle or round) denote disease states
25
26
27
28
29 579 (CT or CD).

30
31
32 580

33
34
35 581 **Figure 2. Functional alterations of the gut microbiota in CD. (a)** Heatmap and hierarchical

36
37 582 clustering of KEGG pathways that are differentially enriched between the microbiota groups
38
39
40 583 identified in Fig 1a. Color scale represents reporter score, and only KEGG pathways with a
41
42 584 reporter score greater than 1.9 are shown. **(b)** Relative abundances of Gram-negative MGS
43
44 585 (the first left panel), Gram-positive MGS (the second left panel), penta-acylated LPS
45
46 586 producing MGS (the middle panel), hexa-acylated LPS producing MGS (the second last
47
48
49 587 panel), and the ratio of hexa- to penta-acylated LPS producing MGS (the last panel) across
50
51
52 588 different groups. The value of relative abundance was log-transformed. **(c)** Relative
53
54
55
56 589 abundances of genes encoding key enzymes for the biosynthesis of different SCFAs across
57
58
59
60
61
62
63
64
65

1 590 different microbiota groups. Carbon monoxide dehydrogenase and acetyl CoA synthase
2
3 591 complex are crucial for acetic acid production; propionyl-CoA transferase and
4
5
6 592 propionyl-CoA/succinyl-CoA transferase are responsible for propionate acid synthesis;
7
8
9 593 butyryl CoA transferase accounts for butyric acid generation. Their relative abundances were
10
11 594 log-transformed. **(b,c)** Statistical comparison by Wilcoxon test followed by a
12
13
14 595 Benjamini-Hochberg correction for significance level; * $q < 0.2$; ** $q < 0.1$; *** $q < 0.05$;
15
16
17 596 **** $q < 0.001$.

18
19
20 597

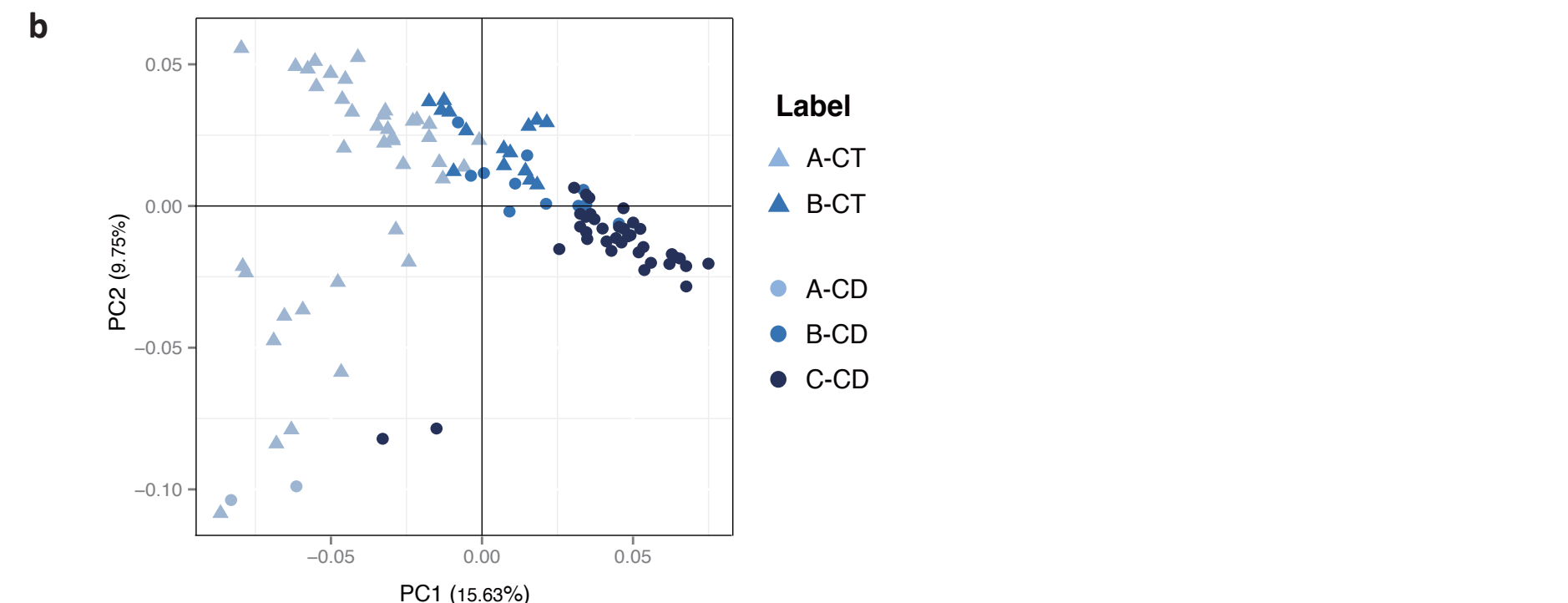
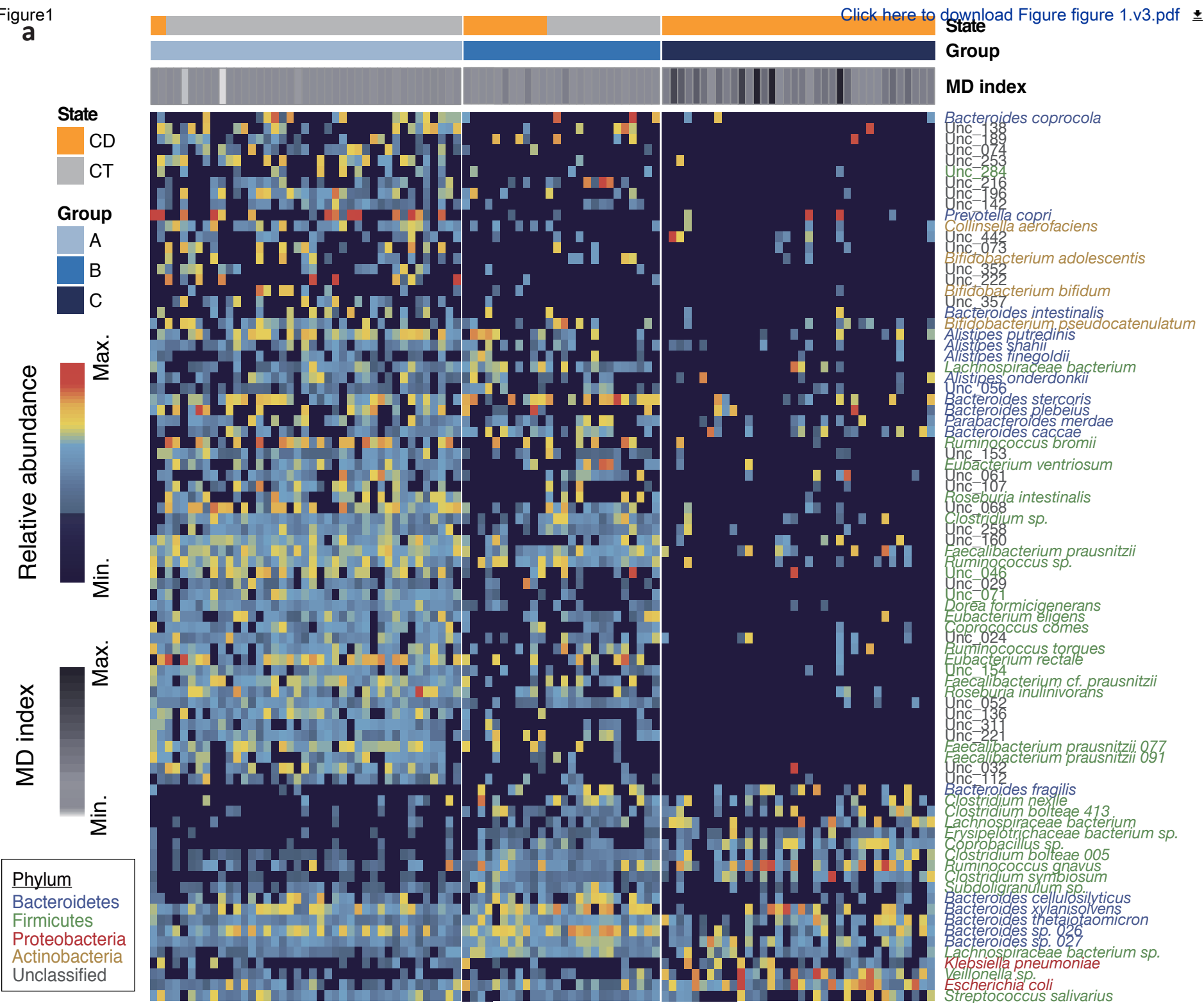
21
22 598 **Figure 3. Reconstruction of microbial interaction networks by CD.** Co-occurrence (blue)
23
24
25 599 relationships and co-exclusion (red) between taxa were estimated by SparCC algorithm, and
26
27
28 600 correlation networks were compared between non-CD samples from metacommunity A (**a**,
29
30
31 601 A-CT) and CD samples from metacommunity C (**b**, C-CD). Only relationships with
32
33
34 602 coefficients above 0.3 are visualized, and the thickness of lines denotes strength of correlation
35
36
37 603 as indicated in the legend. Node size represents mean taxon abundance in networks, and node
38
39
40 604 color represents the growth rate of each species (grey indicates no detection). Taxa of the
41
42 605 same bacterial phylum are encircled by dashed lines.

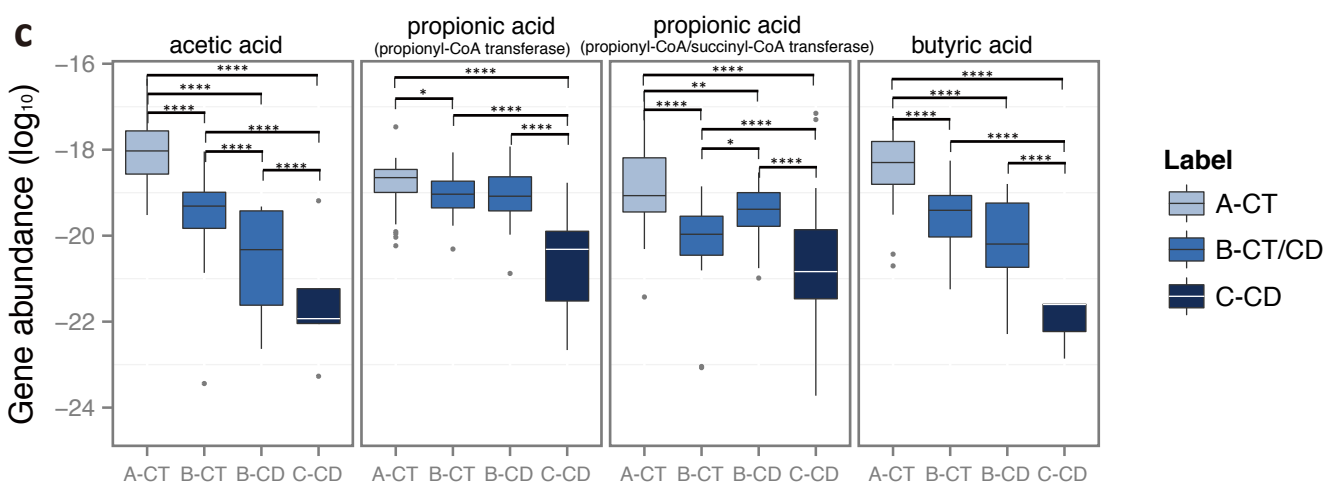
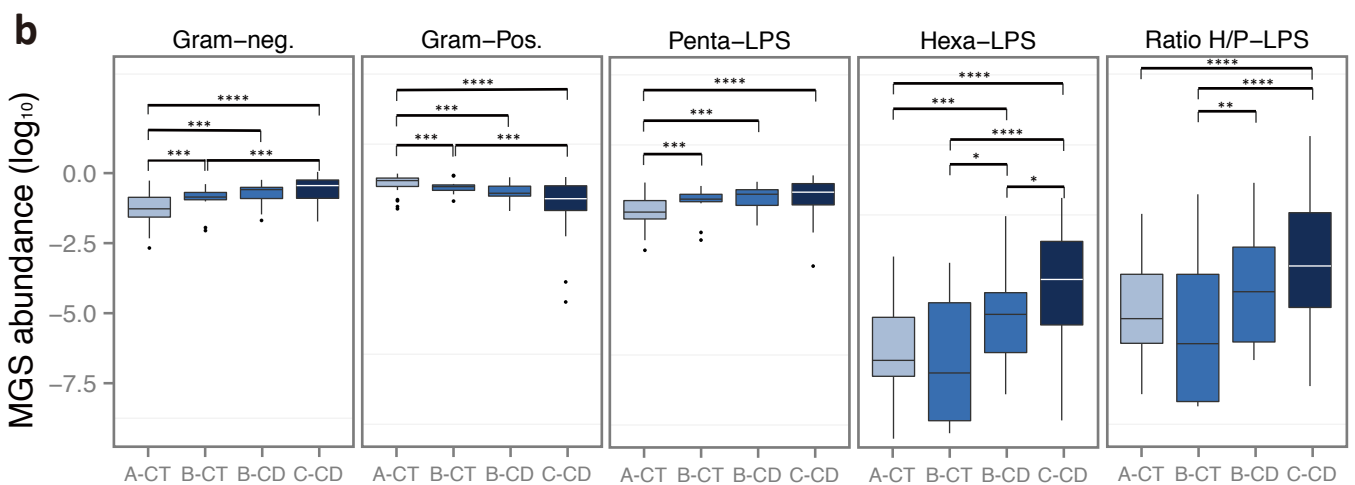
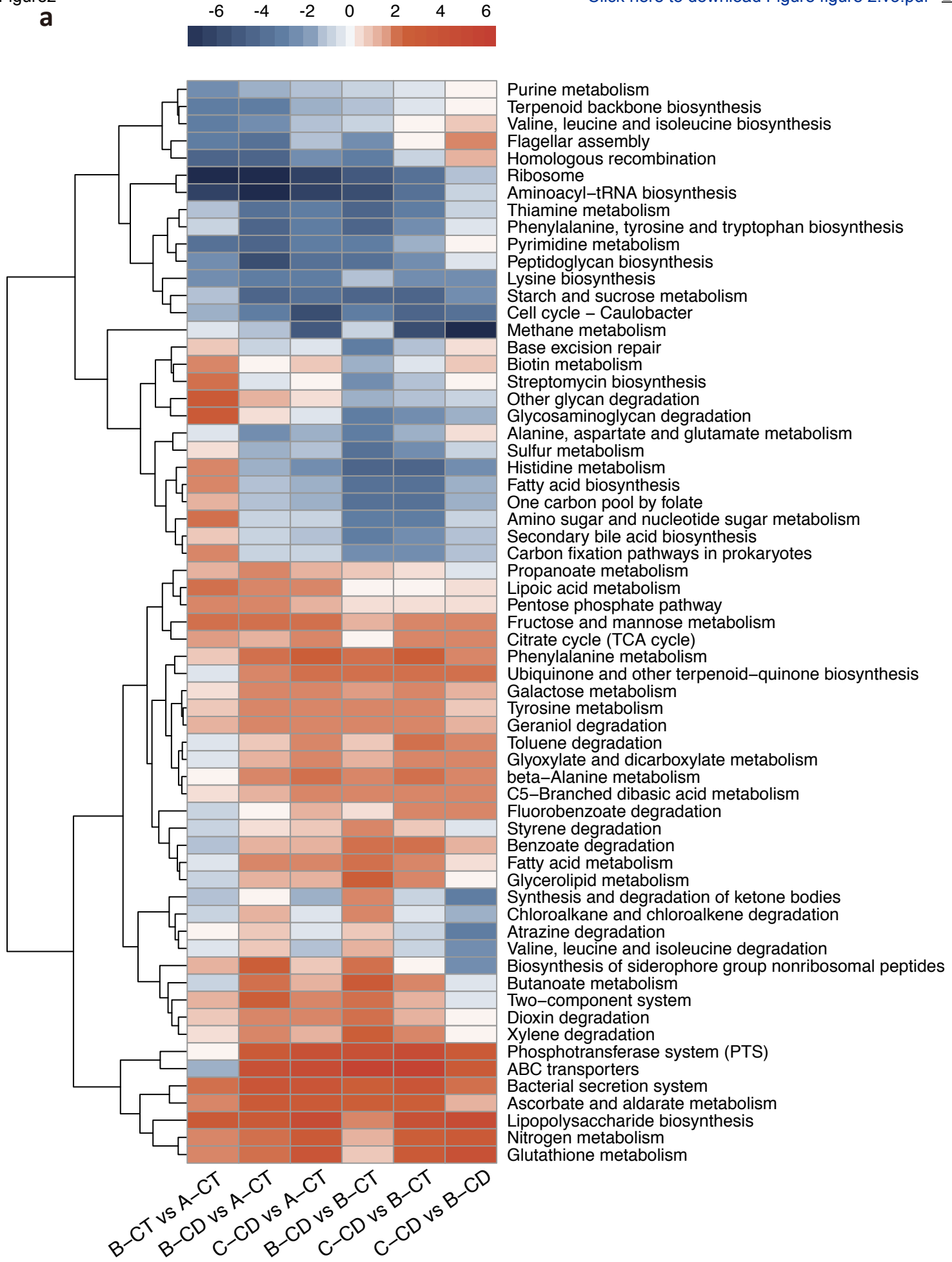
43
44
45 606

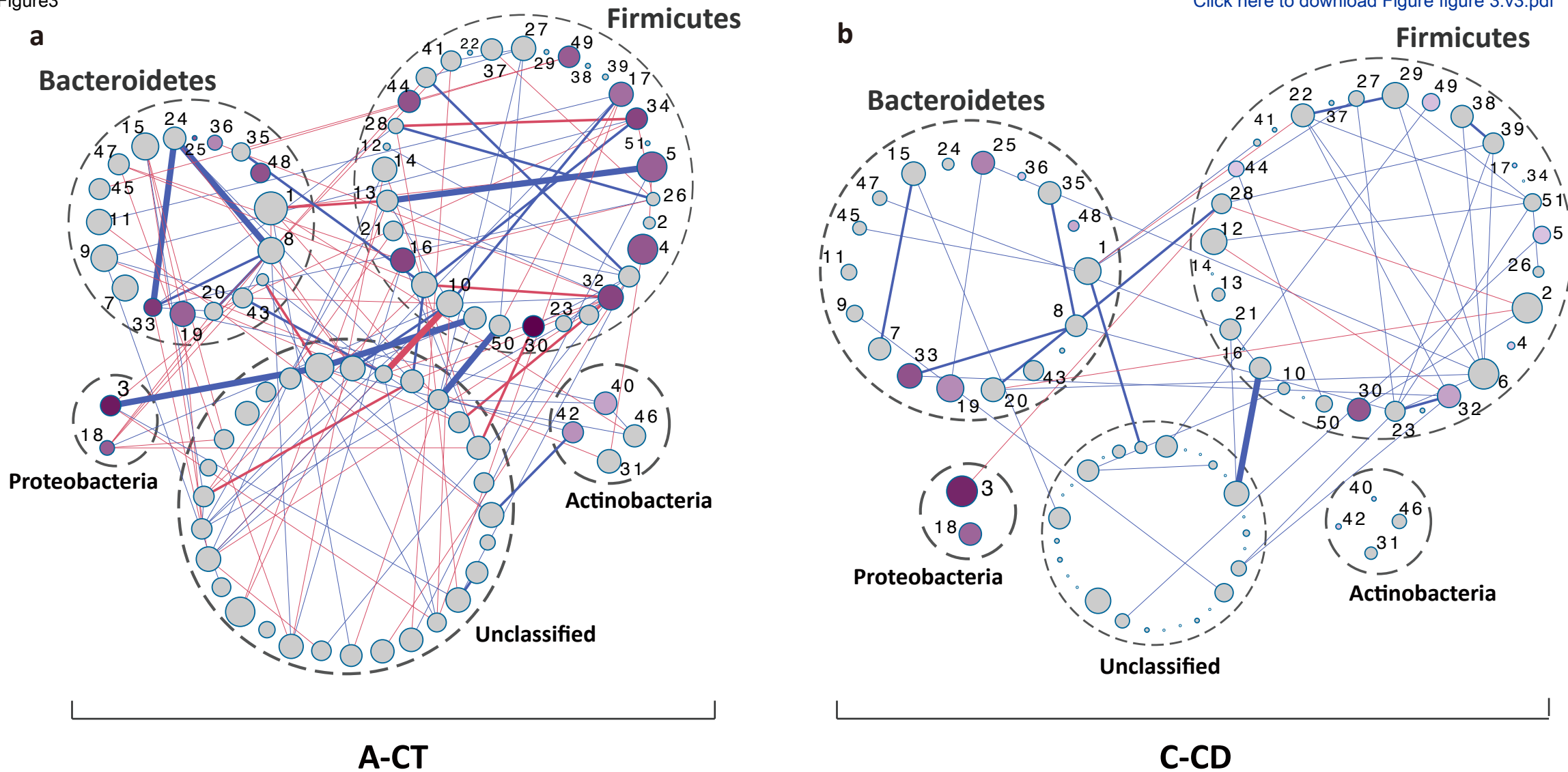
46
47 607 **Figure 4. Moderate modification of CD microbiota by EEN treatment.** **(a)** Gut MGS from
48
49
50 608 CD patients (n=14) before and after 14 days of EEN were clustered into metacommunities
51
52
53 609 and visualized as a heatmap representing the 85 discriminative MGS (as in Fig. 1a). Each
54
55
56 610 column corresponds to one sample. **(b)** PCoA of pre- and post-EEN CD microbiota based on
57
58
59 611 Jensen-Shannon distance (JSD). Arrows indicate the shift of position along the first two

1 612 principal coordinates pre- to post-EEN treatment. The sample whose metacommunity identity
2
3 613 changed after EEN treatment is marked with an asterisk (GZCD029). (c) Heatmap and
4
5
6 614 hierarchical clustering KEGG pathways that were enriched or decreased in post- versus
7
8
9 615 pre-EEN. Color scale represents reporter score, and only KEGG pathways with a reporter
10
11 616 score greater than 1.9 are shown. (d) Log₁₀ relative abundances of Gram-negative MGS (the
12
13 617 first left panel), Gram-positive MGS (the second left panel), penta-acylated LPS producing
14
15 618 MGS (the middle panel), hexa-acylated LPS producing MGS (the second last panel), and the
16
17 619 ratio of hexa- to penta-acylated LPS producing MGS (the last panel) in pre- versus post-EEN.
18
19
20
21
22 620 (e) Log₁₀ relative abundances of genes encoding key enzymes for the biosynthesis of different
23
24 621 SCFAs in pre- versus post-EEN, as calculated in Figure 2c. (d,e) Statistical comparison by
25
26 622 Wilcoxon test followed by a Benjamini-Hochberg correction for significance level showed no
27
28
29
30 623 changes between groups.

31
32
33 624
34
35
36
37
38
39
40
41
42
43
44
45
46
47
48
49
50
51
52
53
54
55
56
57
58
59
60
61
62
63
64
65





1. *Prevotella copri*2. *Veillonella* sp.3. *Escherichia coli*4. *Eubacterium rectale*5. *Ruminococcus bromii*6. *Ruminococcus gnavus*7. *Bacteroides stercoris*8. *Bacteroides* sp. 0269. *Alistipes putredinis*10. *Roseburia inulinivorans*11. *Bacteroides coprocola*12. *Lachnospiraceae* bacterium 10013. *Eubacterium ventriosum*14. *Faecalibacterium* cf. *prausnitzii*15. *Bacteroides plebeius*16. *Faecalibacterium prausnitzii* 07717. *Roseburia intestinalis*18. *Klebsiella pneumoniae*19. *Bacteroides xylanisolvens*20. *Bacteroides* sp. 02721. *Lachnospiraceae* bacterium 06522. *Coprobacillus* sp.23. *Clostridium nexile*24. *Bacteroides cellulosilyticus*25. *Bacteroides fragilis*26. *Subdoligranulum* sp.27. *Ruminococcus* sp.28. *Lachnospiraceae* bacterium sp.29. *Clostridium symbiosum*30. *Streptococcus salivarius*31. *Collinsella aerofaciens*32. *Faecalibacterium prausnitzii* 09434. *Faecalibacterium prausnitzii* 09135. *Bacteroides caccae*36. *Alistipes finegoldii*37. *Coprococcus comes*38. *Clostridium bolteae* 41339. *Clostridium bolteae* 00540. *Bifidobacterium bifidum*41. *Dorea formicigenerans*42. *Bifidobacterium adolescentis*43. *Alistipes onderdonkii*44. *Eubacterium eligens*45. *Bacteroides intestinalis*46. *Bifidobacterium pseudocatenulatum*47. *Parabacteroides merdae*48. *Alistipes shahii*49. *Ruminococcus torques*50. *Clostridium* sp.51. *Erysipelotrichaceae* bacterium sp.

Growth rate



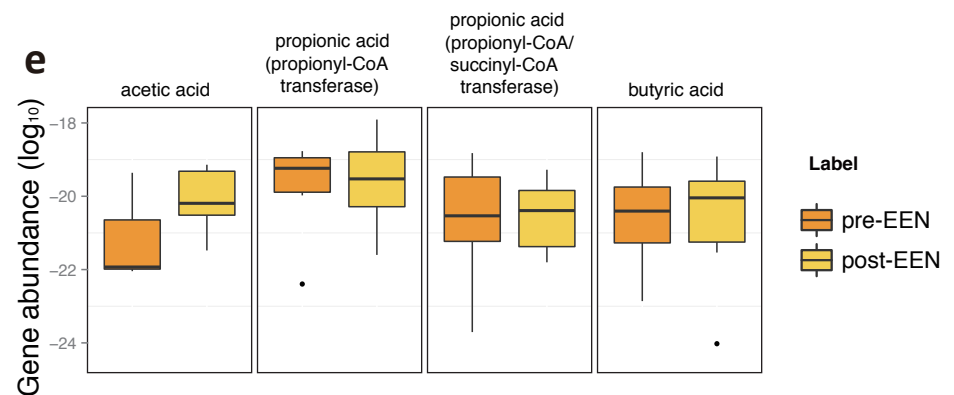
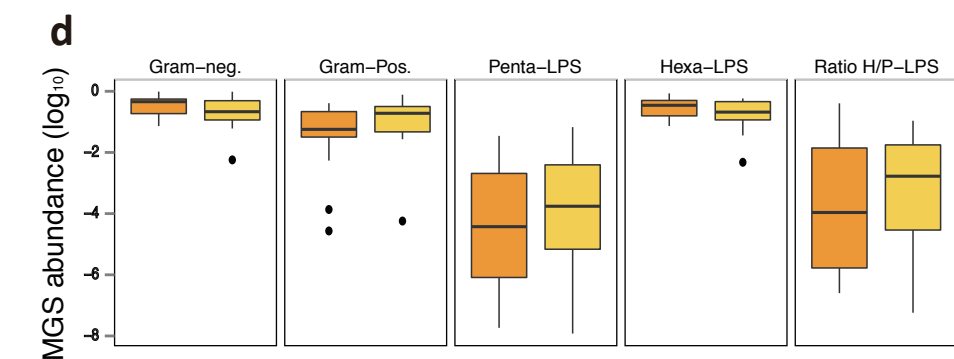
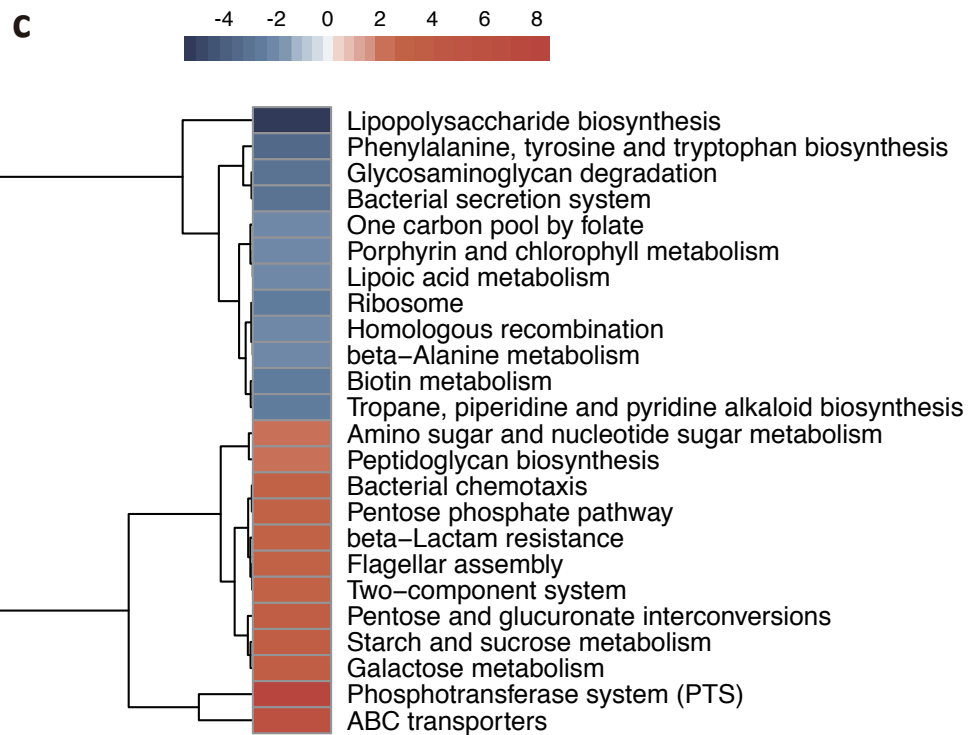
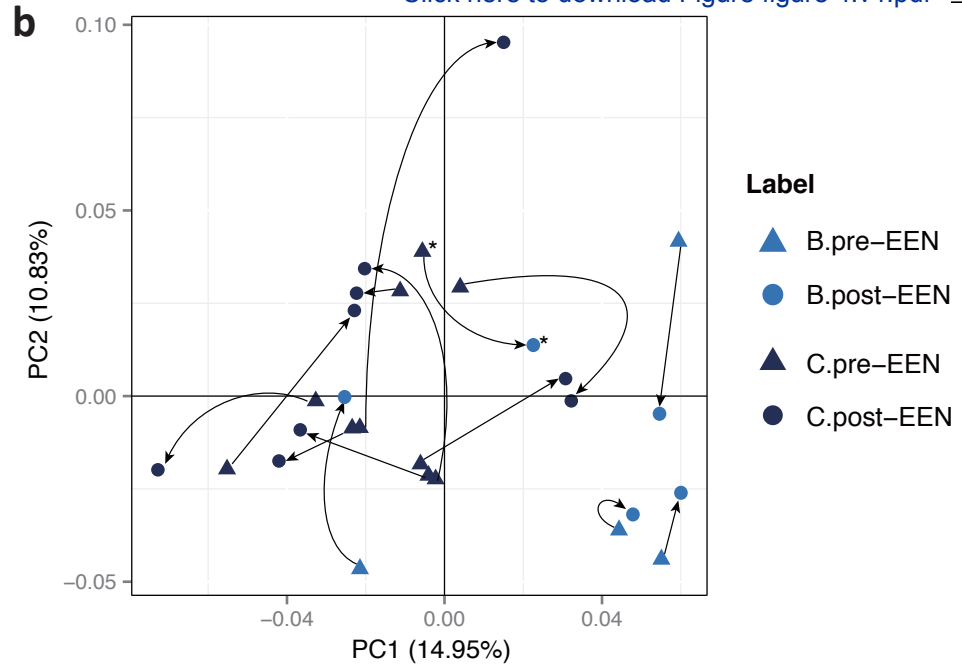
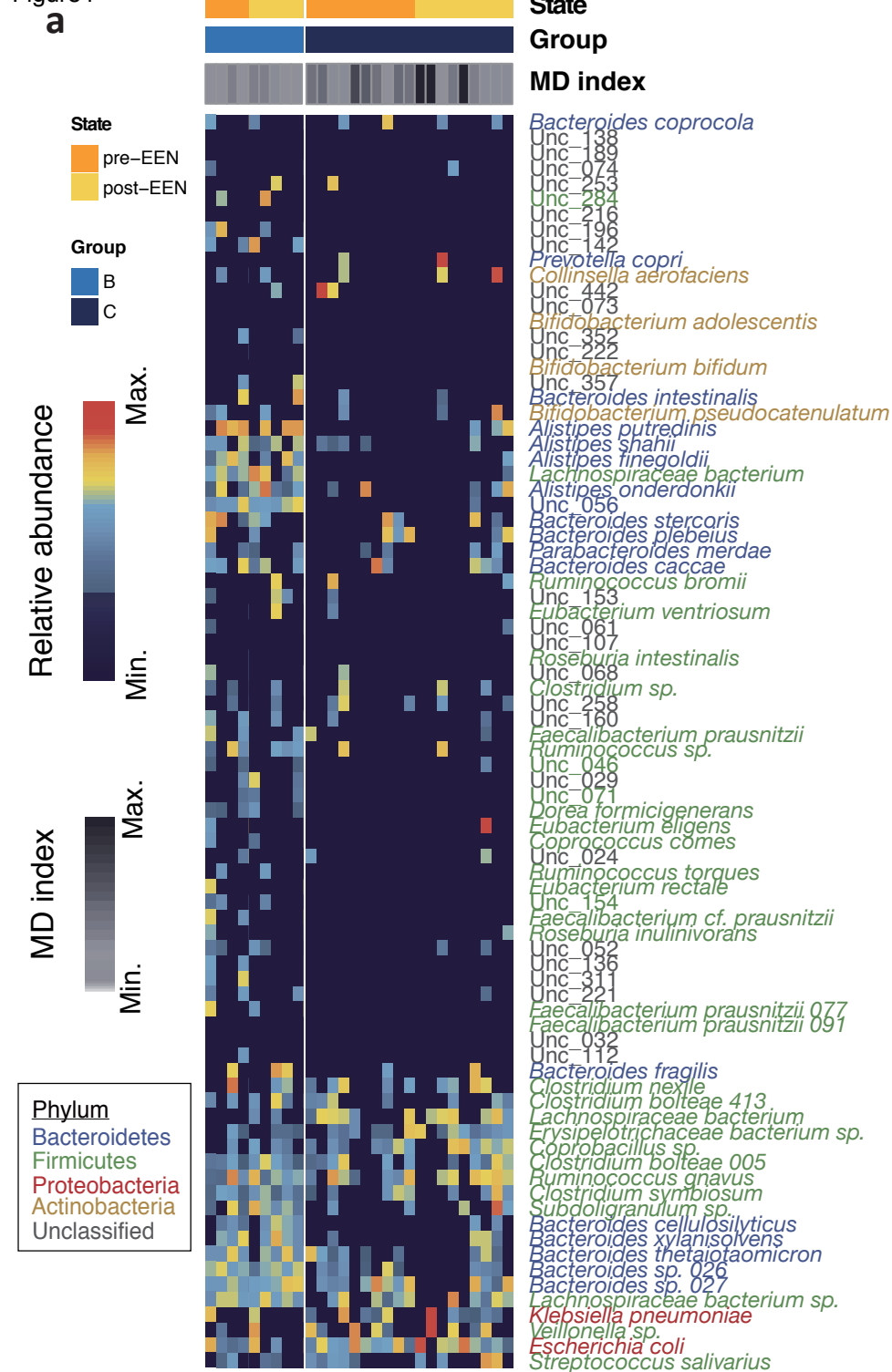
Co-occurring



Co-excluding



Figure 4





Click here to access/download
Supplementary Material
Table & Supplementary Table.CD.xlsx





Click here to access/download
Supplementary Material
SI-CD-paper-gigascience.docx

